FOXA2 enhances anoikis sensitivity in lung adenocarcinoma cells: Dual role of ABCA8 upregulation and NOX4 suppression

NINA HU[1*], LING LI[1*], JIANQING HAO[2], LIFANG LI[1], MENGMENG PAN[1] and JIA HE[1]

[1]Department of Respiratory and Critical Care Medicine, Qingyang People's Hospital, Qingyang, Gansu 745000, P.R. China; [2]State Key Laboratory of Respiratory Diseases, The First Affiliated Hospital of Guangzhou Medical University, Guangzhou Institute of Respiratory Health, National Center for Respiratory Medicine, Guangzhou, Guangdong 510120, P.R. China

Received August 29, 2025; Accepted April 16, 2026

DOI: 10.3892/ol.2026.15777

Abstract. Within the present study, the aim was to investigate the detailed mechanism of forkhead box protein A2 (FOXA2) in anoikis resistance in lung adenocarcinoma (LUAD). The levels of FOXA2 and ATP-binding cassette subfamily A member 8 (ABCA8) were assessed using public databases. The effects of overexpression (oe)-FOXA2, oe-nicotinamide adenine dinucleotide phosphate oxidase 4 (NOX4) and sh-ABCA8 on NOX4 levels, aggregation, cell viability, apoptosis and apoptosis-related proteins were analyzed using reverse transcription quantitative PCR, microscopy, MTT assays, flow cytometry and western blotting. Chromatin immunoprecipitation and dual-luciferase reporter assays were employed to determine the interaction between FOXA2 and ABCA8. In LUAD, FOXA2 and ABCA8 mRNA levels were downregulated, with lower expression observed in in A549 cells compared with BEAS-2B cells; this pattern was pronounced under suspension culture, where A549 cells showed a further decrease in FOXA2/ABCA8 expression alongside a marked increase in NOX4 expression, compared with adherent culture. Furthermore, oe-ABCA8 inhibited NOX4 expression and reversed the effects of oe-NOX4 on enhancing cell aggregation, promoting cell viability, decreasing apoptosis, suppressing cleaved caspase-3 expression and increasing NOX4 level in suspended A549 cells. Furthermore, FOXA2 bound to the ABCA8 promoter region and oe-FOXA2 reversed the effects of ABCA8 silencing on suspended A549 cells, including enhanced cell aggregation, increased cell viability, reduced apoptosis, suppressed cleaved caspase-3 expression and elevated NOX4 expression. Collectively, FOXA2 enhanced ABCA8 transcription, leading to inhibition of NOX4 expression and subsequently alleviating anoikis resistance in A549 cells.

Correspondence to: Dr Ling Li, Department of Respiratory and Critical Care Medicine, Qingyang People's Hospital, 30 Lanzhou Road, Xifeng, Qingyang, Gansu 745000, P.R. China
E-mail: lilingll_222@163.com

*Contributed equally

Key words: anoikis, A549 cells, apoptosis, forkhead box protein A2, anoikis resistance, lung adenocarcinoma, ATP binding cassette subfamily A member 8

Introduction

Lung cancer is one of the leading causes of cancer-related mortalities; there were nearly 2.5 million new cases (12.4% of all cancers in the world), and with an estimated 1.8 million deaths (18.7%) in 2022 (1,2). Non-small cell lung cancer (NSCLC) accounts for >80% of lung cancer cases (3), in which lung adenocarcinoma (LUAD), the most common pathological subtype, constitutes ~40% of lung malignancies (4). Currently, immune checkpoint blockers, including programmed cell death protein 1 (PD-1) and cytotoxic T lymphocyte-associated protein 4, have shown marked clinical progress in the treatment of LUAD (5). In addition, EGFR-targeted tyrosine kinase inhibitors and immunotherapy targeting PD-1 are widely applied in clinical practice (6). However, the 5-year survival rate of patients with LUAD remains low due to factors such as high metastasis rate and resistance to radiotherapy (7). Therefore, an in-depth understanding of the molecular mechanisms underlying the development of LUAD is key in improving the diagnosis and treatment of LUAD.

Immune resistance and tumor metastasis serve key roles in promoting the development of LUAD (8). Anoikis is a programmed cell death process resulting from the loss of cell-extracellular matrix interactions (7). Anoikis resistance allows cancer cells to survive in body circulation, thereby promoting secondary tumor formation in distant organs, which is therefore considered an important mechanism underpinning cancer cell metastasis in NSCLC (9). Notably, there is growing interest in developing LUAD therapeutic strategies aimed at reducing anoikis resistance (10-12).

ATP binding cassette subfamily A member 8 (ABCA8), a member of the ABCA subfamily of transporter proteins, exhibits physiological functions associated with the transport of lipids and cholesterol (13). ABCA8 is lowly expressed in NSCLC and its high expression may improve the overall survival time of patients with lung cancer (14). However, its specific mechanism in lung cancer is not been fully

understood. Nicotinamide adenine dinucleotide phosphate oxidase 4 (NOX4) has been observed to mediate anoikis resistance in lung cancer cells (7). Upregulation of NOX4 not only drives resistance to targeted therapy in lung cancer, but also induces a high expression of programmed death ligand 1 through activating factors such as IL-8, thereby synergistically facilitating immune evasion (8). In colorectal cancer, NOX4 promotes tumor growth, stemness and distant metastasis by activating the MAPK/ERK signaling pathway (15). In addition, ABC transporter-mediated drug efflux and apoptosis escape (including nest-leaving apoptosis resistance) are two core mechanisms underlying cancer treatment resistance (16-18). Based on this, analysis of the Gene Expression Profiling Interactive Analysis (GEPIA) database revealed that ABCA8 was negatively associated with NOX4 in LUAD. Therefore, the present study hypothesized that ABCA8 may be involved in the negative regulation of NOX4 and inhibited anoikis resistance. Forkhead box protein A2 (FOXA2) expression is decreased in the majority of lung cancer cells (19). FOXA2 can also act as a suppressor of tumor metastasis, inhibiting ERK phosphorylation and epithelial mesenchymal transition (EMT) (20). Inhibition of ERK phosphorylation can block the expression of NOX4 (21) and EMT is considered an important factor of anoikis resistance (7). Collectively, it was hypothesized that FOXA2 could inhibit NOX4 expression, thereby attenuating the anoikis resistance of LUAD cells, and that ABCA8 might play a role in this process.

Materials and methods

Attachment culture. Human lung epithelial adenocarcinoma cell line A549 (cat. no. GDC0063) and human lung epithelial normal cell line BEAS-2B (cat. no. GDC0139) were provided by The China Center For Type Culture Collection. All cells were subjected to short tandem repeat analysis and tested negative for *Mycoplasma*. BEAS-2B cells were cultured in keratinocyte-SFM (cat. no. 17005; Invitrogen; Thermo Fisher Scientific, Inc.) with supplements [30 μg/ml bovine pituitary extract (cat. no. abs9119; Absin Bioscience, Inc.) and 0.2 ng/ml rat epidermal growth factor (cat. no. CYT-556; Ameijie Technology Co., Ltd.)]. A549 cells were maintained in RPMI-1640 medium (cat. no. PM150110; Procell Biotechnology Co., Ltd.) containing 10% FBS (cat. no. C0234; Beyotime Biotechnology), 100 U/ml penicillin and 0.1 mg/ml streptomycin (cat. no. 15140122; Gibco; Thermo Fisher Scientific, Inc.). Cell culture was performed in a moist incubator at 37˚C with 5% CO_2.

Suspension culture. Cell culture plates [60 mm; cat. no. CCD06N-060; Belamb Biotechnology (Hangzhou) Co., Ltd.] were coated with 250 μl poly-2-hydroxyethylmethacrylate (poly-HEMA; 50 mg/ml in 95% ethanol; cat. no. P3932; Sigma-Aldrich, Merck KGaA) and dried in a laminar flow hood at room temperature overnight. A549 and BEAS-2B cells were trypsinized into single cell suspensions and $8x10^5$ cells were plated on poly-HEMA-coated dishes. After 24 h, the cells were collected by centrifugation at 300 x g for 5 min at room temperature and processed for cell viability, flow cytometry and protein analyses (22).

Transfection. ABCA8/NOX4/FOXA2 was inserted into the plasmid cytomegalovirus (pCM)-V6-Entry vector (cat. no. PS100001; OriGene Technologies, Inc.) after amplification to construct ABCA8/NOX4/FOXA2 overexpression (oe-) plasmids (oe-ABCA8/oe-NOX4/oe-FOXA2) and the empty vector served as the negative control (NC). In addition, short hairpin RNA (shRNA) targeting ABCA8 (sh-ABCA8; cat. no. C02001; 5'-AAGTCAAATAGT TAAAGCAAATT-3') and shRNA targeting NC (sh-NC, 5'-TTCTCCGAACGTGTCACGT-3') were purchased from Shanghai GenePharma Co., Ltd. These shRNA constructs were cloned into the pGPU6 vector backbone. The pGPU6 vector contains a U6 promoter for shRNA expression and a neomycin resistance gene for selection in mammalian cells. The plasmid sequence is listed in Supplementary Data 1. Following the manufacturer's instructions of Lipo6000™ transfection reagent (Lipo6000; cat. no. C052; Beyotime Biotechnology), $3x10^5$ A549 cells were seeded in a 96-well plate (Biovision, Inc.). Simultaneously, Lipo6000 (0.2 μl) was diluted with 5 μl DMEM (cat. no. PM150210; Procell Biotechnology Co., Ltd.) without serum. A total of 100 ng oe-ABCA8/oe-NOX4/oe-FOXA2 or sh-ABCA8/sh-NC was diluted with 5 μl serum-free DMEM (1:1 ratio). After 20 min, Lipo6000 and oe-ABCA8/oe-NOX4/oe-FOXA2 and/or sh-ABCA8/sh-NC was introduced to the A549 cell culture medium for co-culture at 37˚C for 6 h. Subsequently, the whole culture medium was replaced with a fresh complete medium for additional 24 h of culture. Transfection efficiency was detected through reverse transcription quantitative PCR (RT-qPCR) and western blotting.

Cell grouping and treatment. First, A549 and BEAS-2B cells were divided into attachment (Att) and suspension (Sus) groups and received attachment or suspension culture as aforementioned. Second, A549 cells were assigned to Control (without treatment), oe-NC (transfected with oe-NC) or oe-ABCA8 (transfected with oe-ABCA8) groups. Third, A549 cells were distributed to Control, oe-NC and oe-NOX4 groups to validate the transfection efficiency. Fourth, A549 cell suspension was assigned to oe-NC, oe-NOX4, oe-ABCA8 and oe-NOX4 + oe-ABCA8 groups, where transfection with NC, oe-NOX4, oe-ABCA8 and oe-NOX4 + oe-ABCA8 was performed. Fifth, A549 cells were divided to Control, oe-NC (transfected with oe-NC) and oe-FOXA2 (transfected with oe-FOXA2) groups. Sixth, A549 cells were distributed into Control, sh-NC (transfected with sh-NC) and sh-ABCA8 (transfected with ABCA8) groups. Seventh, A549 cell suspension was divided into Control (no treatment), sh-ABCA8, oe-FOXA2 and sh-ABCA8 + oe-FOXA2 groups and cells in the last 3 groups were separately transfected with sh-ABCA8, oe-FOXA2 and sh-ABCA8 + oe-FOXA2.

Bioinformatics analysis. Prediction of FOXA2 and ABCA8 expressions in LUAD based on the sample types (normal n=59; primary tumor n=515) was achieved by searching the The University of Alabama at Birmingham Cancer data analysis portal (UALCAN) (23). $P<0.05$ was considered statistically significant. GEPIA (http://gepia.cancer-pku.cn/; version 2.0) was used for predicting the association between ABCA8 and NOX4 or between ABCA8 and FOXA2 in LUAD. In addition,

FOXA2 was identified as an upstream binding transcription factor of ABCA8 from the hTFtarget database (guolab.wchscu.cn/hTFtarget/#!/; version 1.0) (24). Subsequently, the University of California Santa Cruz (http://genome.ucsc.edu/; version 1.0) and JASPAR database (https://jaspar.genereg.net/; 2024 update) were employed to obtain the predicted binding sites of FOXA2 in the ABCA8 promoter region. Default parameters were used for transcription factor binding site prediction in JASPAR, with a relative profile score threshold of >80% for high-confidence predictions.

Chromatin immunoprecipitation (ChIP) assay. Enrichment of FOXA2 in ABCA8 promoter region was evaluated with ChIP kit (cat. no. P2078; Beyotime Biotechnology). After fixation in formaldehyde (1%; cat. no. BTN160220; Beijing Bio-Lab Technology Co., Ltd.) at 37˚C for ~10 min, the A549 cells were treated with glycine (125 mM; cat. no. HY-Y0966; MedChemExpress) and lysed in 1 mM PMSF (cat. no. 10837091001; Sigma-Aldrich; Merck KGaA) added with SDS lysis buffer (cat. no. P0013G; Beyotime Biotechnology). To obtain the genome at the size of 200-1,000 bp, the lysate was sonicated on ice (10 sec pulse and 50 sec break, six times; 20% amplitude). A total of 20 ml sonicated lysate was taken as input for subsequent testing and 2 ml sonicated lysate was centrifuged at 10,000 x g (5 min; 4˚C) with 70 ml Protein A + G Agarose/Salmon Sperm DNA. The supernatant was removed for measurement. Next, ChIP dilution buffer containing 1 mM PMSF was prepared and added to dilute the sonically processed lysate. The cross-linked chromatin lysates were incubated with FOXA2 antibody (1:5; cat. no. ab256493; Abcam) and HRP-goat anti-rabbit IgG (H+L; 1:500; cat. no. ab205718; Abcam) at 4˚C overnight. A total of 60 μl Protein A + G Agarose/Salmon Sperm DNA was added and slowly mixed for 1 h to precipitate the primary antibody-recognized protein or corresponding complex. The mixture was then centrifuged again as before and was washed with the following buffers: Low-salt immune complex washing buffer (x1); high-salt immune complex washing buffer (x1); LiCl immune complex washing buffer (x1); Tris-EDTA buffer (x2). Endogenous DNA-protein compounds were precipitated by protein agarose/agarose and de-crosslinked overnight at 65˚C. Finally, DNA components were extracted by the standard phenol-chloroform method (25). RT-qPCR was performed to detect the enrichment of FOXA2 in the promoter region of ABCA8. The primer sequences were as follows: Forward (5'-GCTTTCTATGTCCACCGCCT-3'); and reverse (5'-AGCCCATCCAGCATTCAACA-3'). The results were analyzed with Image J software (version 1.53; National Institutes of Health).

Dual-luciferase reporter assay. Wild-type (WT-pcDNA-FOXA2) and mutant FOXA2 (MUT-pcDNA-FOXA2) were cloned into the pGL3-basic plasmid (E1751; Promega Corporation) to construct the luciferase reporter vectors, with the empty pGL3-Basic plasmids (WT/MUT-Empty vector) serving as the NC. The *Renilla* luciferase reporter vector pRL-SV40 (cat. no. E2231; Promega Corporation) were regarded as an internal control. The recombinant plasmids were co-transfected into A549 cells for 36 h. Then, the cells were lysed in 100 μl passive lysis buffer (cat. no. E1941; Promega Corporation). Luciferase activity in cell lysates was detected with a Dual Luciferase® Reporter Assay System (cat. no. E1910; Promega Corporation) (26).

RT-qPCR. Total RNA from BEAS-2B/A549 cells were extracted with NucleoSpin® RNA Plus kit (cat. no. 740984.50; Machery-Nagel GmbH). To determine the quantity of the isolated RNA, a NanoDrop™ 2000 spectrophotometer (cat. no. ND-2000; Thermo Fisher Scientific, Inc.) was employed. RT and amplification of the RNAs were performed utilizing the One-Step RT-qPCR Kit (cat. no. P4305; Beijing Genenode Biotech Co., Ltd), according to the manufacturer's instructions. The reaction was performed on a CFX384 Touch PCR detection system (cat. no. 1855195; Bio-Rad Laboratories, Inc.) under the following conditions: 42˚C for 30 min, 94˚C for 2 min, followed by 40 cycles of 94˚C for 20 sec, 60˚C for 20 sec, and 72˚C for 20 sec. The expression level was calculated using $2^{-\Delta\Delta Cq}$ method (27) with GAPDH as the internal reference. The relative primers are listed in Table I.

Confocal microscopy imaging. A549 cell suspension was prepared, dripped onto a microslide and covered with a coverslip. Confocal microscopy imaging was performed on a Zeiss LSM 510 laser scanning microscope (magnification, x100; Zeiss GmbH).

MTT assay. A549 cells in suspension culture were seeded into 96-well plate at a density of $3x10^5$/well and were incubated at 37˚C for 24 h. The culture medium was then discarded and the cells were incubated with 20 μl MTT reagent (5.0 mg/ml; cat. no. ab211091, Abcam) for 4 h at 37˚C. The medium solution was removed. Next, 100 μl DMSO (cat. no. ST038; Beyotime Biotechnology Co., Ltd.) was added to the wells. A microplate reader (cat. no. 1681130; Bio-Rad Laboratories, Inc.) was exploited to evaluate absorbance at 590 nm (28).

Flow cytometry. A549 apoptosis in suspension culture was monitored using the Annexin V-FITC/PI Apoptosis Detection Kit (cat. no. 40302ES50; Shanghai Yeasen Biotechnology Co., Ltd.). Following the instructions of the kit, A549 cells were centrifuged at 300 x g for ~5 min (at 4˚C) and the cell culture medium was removed. Cells were washed with PBS and counted. Subsequently, 100 μl binding buffer was added to the wells, followed by addition of 5 μl Annexin V-FITC and 10 μl PI staining solution. The cells were then cultured in an incubator at 25˚C for 10 min (in the dark). Next, 400 μl binding buffer was added to the cells, which were then placed in an ice bath. The results were assessed using a FACSCalibur flow cytometer (BD Biosciences) with FlowJo software (version 10; FlowJo, LLC).

Western blotting. With lysis buffer (cat. no. 20118ES60; Shanghai Yeasen Biotechnology Co., Ltd.), the protein was isolated from A549 cells. Then, the extracted lysates underwent 5 min centrifugation (1,000 x g) at 4˚C and the supernatant was obtained for following detection. A BCA assay kit (cat. no. 23225; Thermo Fisher Scientific, Inc.) was exploited to determine the protein concentration. Then, SDS-PAGE gel electrophoresis (8-12%; cat. no. M00659;

Table I. Primers for reverse transcription-quantitative PCR.

Gene	Forward primer, 5'→3'	Reverse primer (5'-3')
FOXA2	CATGCACTCGGCTTCCAGTA	GCGAGATGTACGAGTAGGGC
ABCA8	GTGTCAACAAACTTGGGCCTT	CAGGCCGGTGAGGAAAGATT
NOX4	CAGTCTTTGACCCTCGGTCC	TGATCCTCGGAGGTAAGCCA
GAPDH	GACAGTCAGCCGCATCTTCT	GCGCCCAATACGACCAAATC

FOXA2, forkhead box protein A2; ABCA8, ATP-binding cassette subfamily A member 8; NOX4, nicotinamide adenine dinucleotide phosphate oxidase 4.

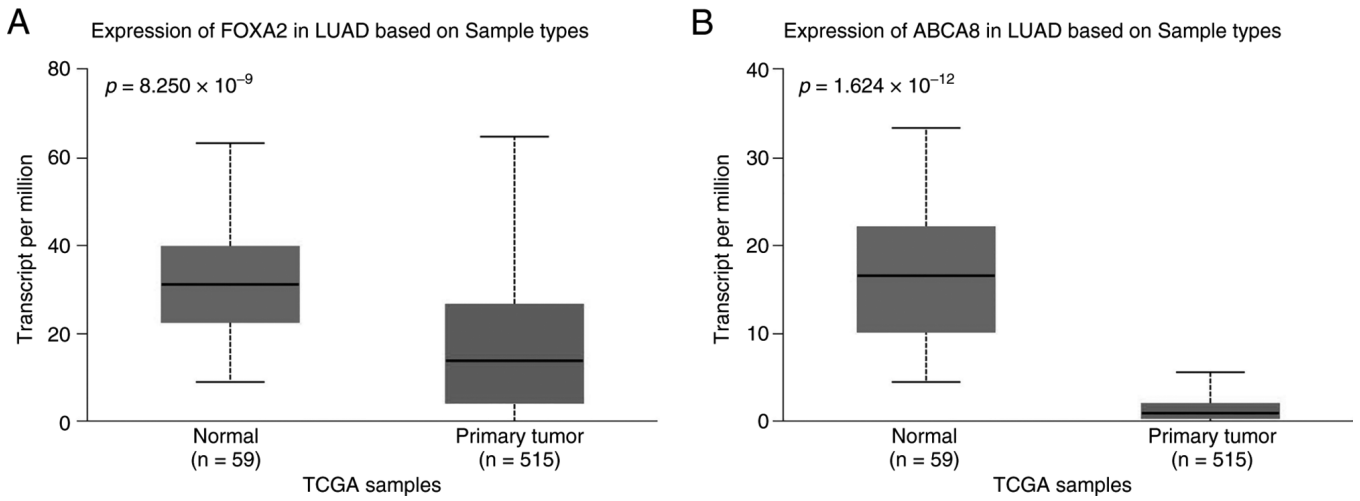

Figure 1. FOXA2 and ABCA8 expression levels are downregulated in LUAD. (A) The University of Alabama at Birmingham Cancer data analysis portal was used to predict FOXA2 ($P=8.250x10^{-9}$) and (B) ABCA8 ($P=1.624x10^{-12}$) expression levels in LUAD based on the sample types (normal n=59; primary tumor n=515). FOXA2, forkhead box protein A2; ABCA8, ATP binding cassette subfamily A member 8; LUAD, lung adenocarcinoma; TCGA, The Cancer Genome Atlas.

GenScript Biotech Corporation) was applied for electrophoresis of equal amount of protein (30 μg/lane), which was immediately loaded onto PDVF membranes (cat. no. MSPVDF022BX, Membrane Solutions). Next, the membranes were blocked (10 min) with 10% blocking buffer (cat. no. YT067; Beijing Biolab Technology Co., Ltd.) at room temperature and probed with primary antibodies for NOX4 (cat. no. ab154244; 67 kDa; 1:500; Abcam), cleaved-caspase3 (cat. no. ab32042; 17 kDa; 1:500; Abcam), cleaved caspase-8 (cat. no. 9496; 1:1,000; 25 kDa; Cell Signaling Technology, Inc.), caspase3 (cat. no. ab32351; 31 kDa; 1:5,000; Abcam), caspase8 (cat. no. ab25901; 55 kDa; 1 μg/ml; Abcam), ABCA8 (cat. no. ab230896; 179 kDa; 1:1,000; Abcam) and GAPDH (cat. no. 5174; 37 kDa; 1:1,000; Cell Signaling Technology, Inc.) at 4˚C overnight. Subsequently, the membranes were exposed to HRP-secondary antibody goat anti-rabbit IgG H&L (cat. no. ab6721; 1:2,000; Abcam) for 1 h at room temperature. The membranes with proteins were then visualized using ECL Plus (cat. no. WBKlS0100; MilliporeSigma; Merck KGaA) and exposed using the Kodak In-Vivo Imaging System FX Pro (Kodak). The results were analyzed with a semi-quantification software (Image J; version 1.53; National Institutes of Health) and GAPDH served as the internal reference.

Statistical analysis. All measurement data are presented as mean ± SD. Comparisons between two groups were performed by independent sample t-tests, while comparisons among multiple groups were made through ANOVA tests. The normality of data distribution was verified using the Shapiro-Wilk test and the homogeneity of variances was assessed with the Brown-Forsythe test. Statistical analyses were achieved using GraphPad software (version 8.0; Dotmatics) and $P<0.05$ was considered to indicate a statistically significant difference.

Results

FOXA2 and ABCA8 expression levels are downregulated in LUAD. Given that ABCA8 expression is downregulated in NSCLC (13), a series of experiments were conducted to reveal its associated pathways in LUAD mechanisms. Through retrieval and assessment of the UALCAN website, expression levels of FOXA2 and ABCA8 in LUAD were predicted based on sample type (normal n=59; primary tumor n=515). FOXA2 expression was decreased in LUAD tumor tissues, compared with normal tissues ($P=8.250x10^{-9}$; Fig. 1A) and this was also true for ABCA8 expression in LUAD tumor tissues ($P=1.624x10^{-12}$; Fig. 1B). These findings indicated that

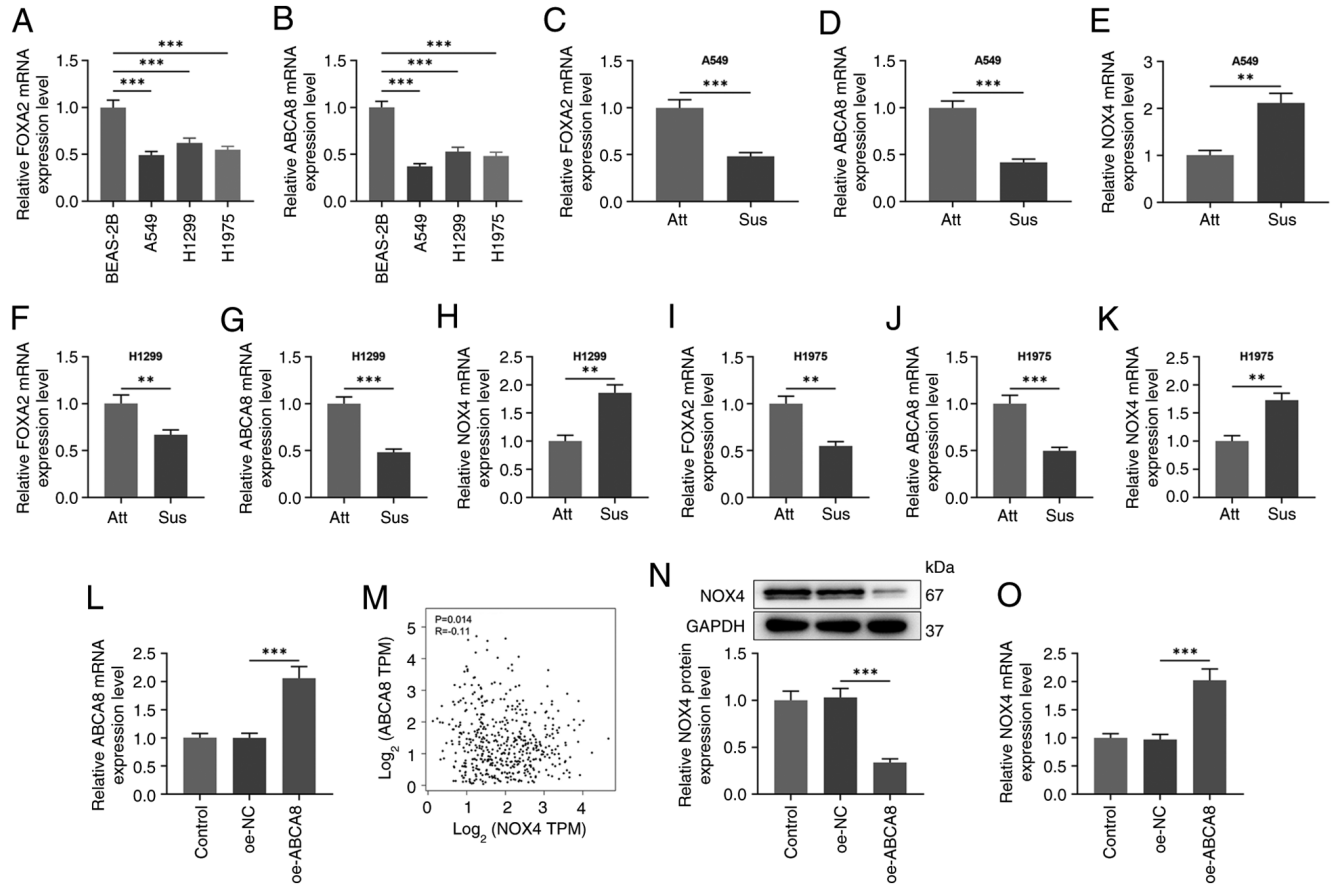

Figure 2. ABCA8 overexpression reduces anoikis resistance in A549 cells by inhibiting NOX4 expression. BEAS-2B cells, A549 cells, H1299 cells and H1975 cells were divided into Att and Sus groups and received attachment culture or suspension culture. RT-qPCR was conducted to detect mRNA levels of (A) FOXA2 and (B) ABCA8 in BEAS-2B cells, A549 cells, H1299 cells and H1975 cells undergoing attachment culture, with GAPDH serving as the internal reference. Relative mRNA levels of (C) FOXA2, (D) ABCA8 and (E) NOX4 in A549 cells, relative mRNA levels of (F) FOXA2, (G) ABCA8 and (H) NOX4 in H1299 cells and relative mRNA levels of (I) FOXA2, (J) ABCA8 and (K) NOX4 in H1975 cells were measured (in both Att and Sus culture) by RT-qPCR, with GAPDH serving as the internal reference. (L) A549 cells were assigned into Control (without treatment), oe-NC (transfected with oe-NC) and oe-ABCA8 (transfected with oe-ABCA8) groups. The mRNA expression of ABCA8 was determined using RT-qPCR, with GAPDH serving as the internal reference. (M) Gene Expression Profiling Interactive Analysis was used for prediction of the association between ABCA8 and NOX4 (P=0.014; R=-0.11). (N) The protein expression of NOX4 was determined using western blotting, with GAPDH serving as the internal reference. (O) A549 cells were divided into Control (without treatment), oe-NC (transfected with oe-NC) and oe-NOX4 (transfected with oe-NOX4) groups. The mRNA expression of NOX4 was measured using RT-qPCR, with GAPDH serving as the internal reference. Data are presented as the mean ± SD (n=3). There were three biological replicates in each experimental group. **P<0.01 and ***P<0.001. FOXA2, forkhead box protein A2; ABCA8, ATP binding cassette subfamily A member 8; NOX4, nicotinamide adenine dinucleotide phosphate oxidase 4; Att, attachment; Sus, suspension; oe, overexpression; NC, negative control; RT-qPCR, reverse transcription-quantitative PCR; TPM, transcripts per million.

both FOXA2 and ABCA8 expression levels were decreased in LUAD.

ABCA8 and FOXA2 expression levels are decreased in A549 cells, H1299 cells and H1975 cells and NOX4 is negatively associated with ABCA8. Anoikis resistance has been established as a key process of cancer cell metastasis in LUAD (29). NOX4 can mediate anoikis resistance in lung cancer cells (7). Considering the existing results and the established downregulation of ABCA8 and FOXA2 in LUAD, the association between ABCA8 and NOX4 in the anoikis resistance of LUAD was determined. Suspension culture was carried out for A549 cells, H1299 cells, H1975 cells and BEAS-2B cells to induce the anoikis resistance, with an attachment culture serving as the control. Subsequently, RT-qPCR was conducted to detect the mRNA expression of FOXA2 and ABCA8 in A549 cells and BEAS-2B cells undergoing attachment culture. Compared with BEAS-2B cells, A549 cells, H1299 cells and H1975 cells presented levels of FOXA2 and ABCA8 decreased by ~50% (P<0.001; Fig. 2A and B). Then, mRNA levels of FOXA2, ABCA8 and NOX4 in A549 cells, H1299 cells and H1975 cells experiencing attachment and suspension culture were measured. The results revealed that ABCA8 and FOXA2 levels in A549 cells, H1299 cells and H1975 cells were lower in suspension culture compared with attachment culture (P=0.0007, P=0.0003, P=0.005, P=0.0004, P=0.001 and P=0.0008; Fig. 2C, D, F, G, I and J). Conversely, A549 cells, H1299 cells and H1975 cells in suspension culture exhibited higher NOX4 mRNA level compared with those in attachment culture (P=0.0011, P=0.0011 and P=0.0013; Fig. 2E, H and K). Subsequently, RT-qPCR data reflected that oe-ABCA8 significantly increased ABCA8 expression by 1-fold in A549 cells (P=0.0002; Fig. 2L), which demonstrated successful transfection. Before experiments, a negative correlation was predicted between ABCA8 and NOX4 in GEPIA (P=0.014; R=-0.11; Fig. 2M), which was further determined by western blotting

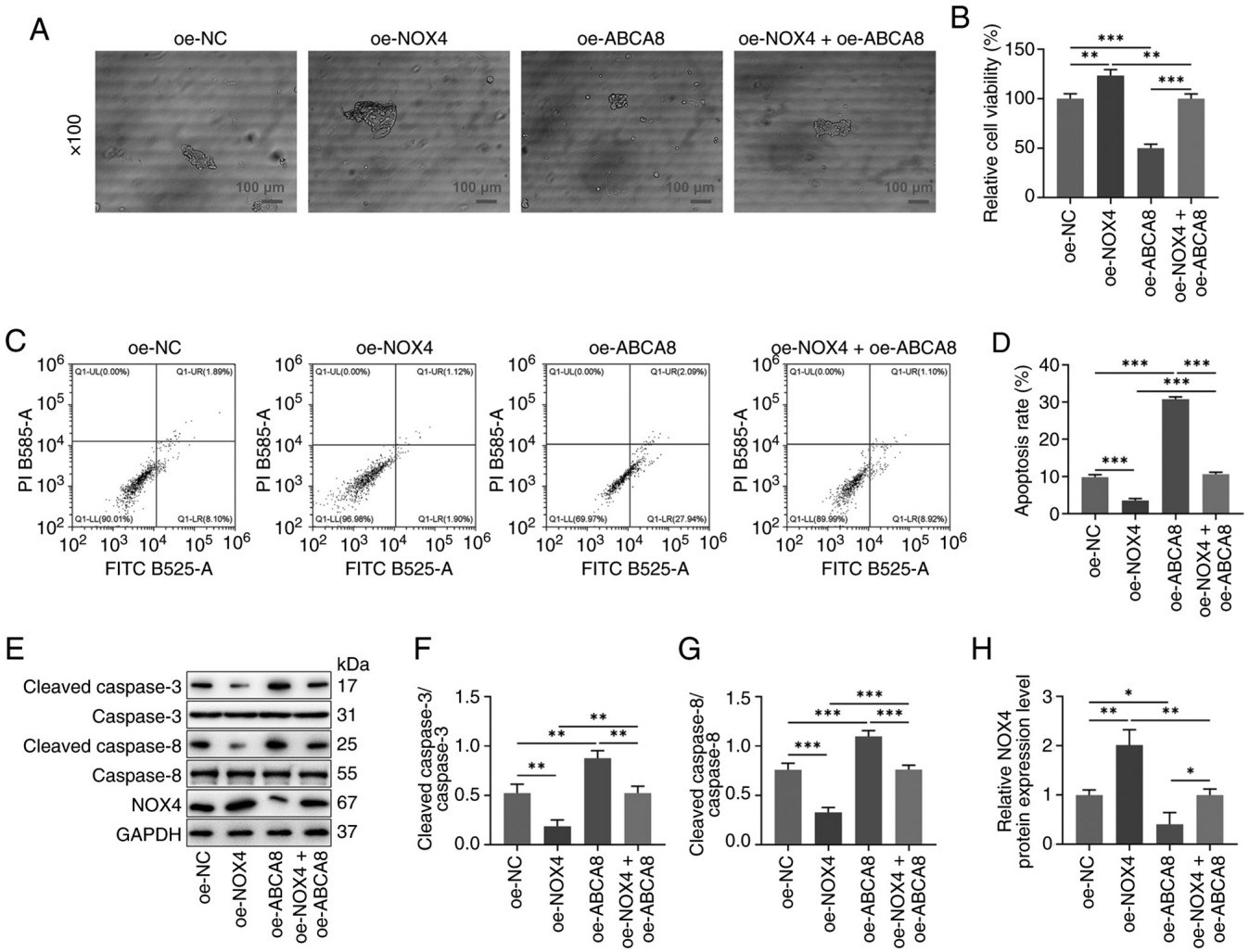

Figure 3. Effects of NOX4 or ABCA8 overexpression on cell viability, apoptosis rate and apoptosis-associated protein levels. (A) A549 cells in suspension culture were assigned to oe-NC, oe-NOX4, oe-ABCA8 (treated as before) and oe-NOX4 + oe-ABCA8 (transfected with oe-NOX4 and oe-ABCA8) groups. Confocal microscopy images were obtained from a microscope (magnification, x100; scale bar, 100 μm). (B) Viability of A549 cells (suspension culture) was monitored by MTT assay. (C) Flow cytometry was employed to determine and (D) quantify the apoptosis in A549 cells (suspension culture). (E) Western blotting measured (F) cleaved-caspase3, caspase3, (G) cleaved-caspase8, caspase8 and (H) NOX4 protein expressions in A549 cell suspension, with GAPDH serving as the internal reference. Data are presented as the mean ± SD (n=3). There were three biological replicates in each experimental group. *P<0.05, **P<0.01 and ***P<0.001. ABCA8, ATP binding cassette subfamily A member 8; NOX4, nicotinamide adenine dinucleotide phosphate oxidase 4; oe-, overexpression; NC, negative control.

results. Furthermore, oe-ABCA8 decreased NOX4 protein expression by ~70% (P=0.0001; Fig. 2N). Collectively, it was concluded that FOXA2 and ABCA8 levels were downregulated in A549 cells and a further reduction could be induced in A549 cells under suspension suspension; correspondingly, NOX4 expression was upregulated and exhibited a negative correlation with ABCA8 level.

Oe-ABCA8 mitigated anoikis resistance in A549 cells by inhibiting NOX4 expression. Subsequently, oe-NOX4 plasmid was transfected into A549 cell to ascertain the negative association between ABCA8 and NOX4. From the RT-qPCR results, it was noted that oe-NOX4 successfully increased the NOX4 mRNA level in A549 cells (P=0.0002; Fig. 2O). Then, confocal microscopy images substantiated that oe-NOX4 promoted the aggregation of A549 cells, which was reversed by oe-ABCA8 (Fig. 3A). In addition, MTT assay results indicated that oe-ABCA8 attenuated the stimulatory effect of NOX4 on A549 cell viability by ~20% (P=0.002; Fig. 3B). According to the outcomes of flow cytometry, it was observed that oe-NOX4 reduced apoptosis rate of A549 cells by ~63% (P<0.0001; Fig. 3C and D), which was offset by oe-ABCA8 (P<0.0001; Fig. 3C and D). In addition, the expressions of cleaved-caspase3 and cleaved-caspase8, established apoptosis-associated proteins (30), as well as NOX4 expression were determined using western blotting. The relative protein expression of cleaved-caspase3 and cleaved-caspase8 in A549 cells was reduced by ~50% after transfection of oe-NOX4 (P=0.0028 and P<0.0001; Fig. 3E-G), whereas oe-ABCA8 reversed this inhibitory effect of oe-NOX4 (P=0.0028 and P<0.0001; Fig. 3E-G). NOX4 expression in A549 cells was upregulated by oe-NOX4, yet downregulated by oe-ABCA8 (P=0.0018 and P=0.0018; Fig. 3E-H). Overall, oe-NOX4 strengthened anoikis resistance in LUAD (A549) cells, which was counteracted by oe-ABCA8.

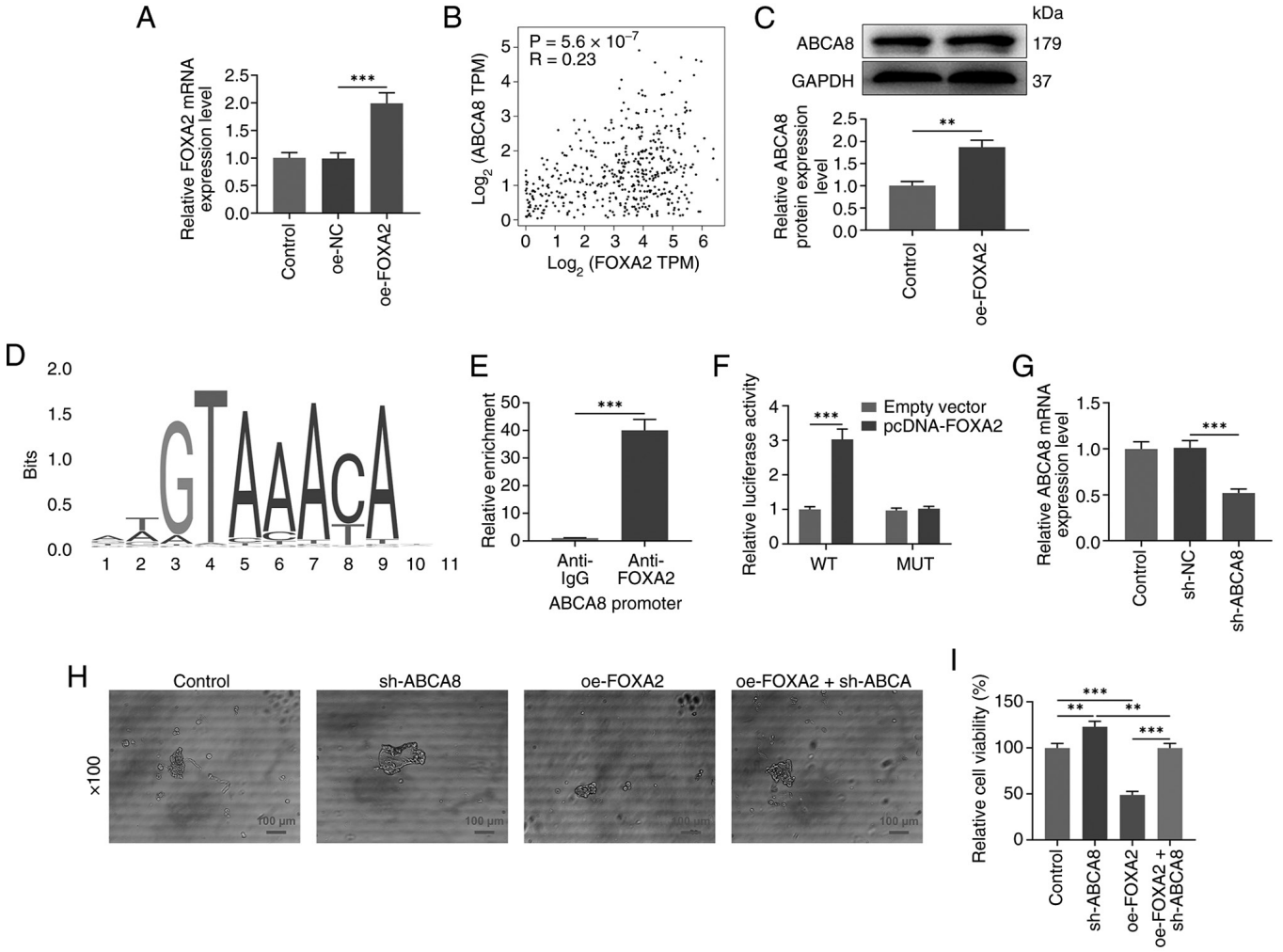

Figure 4. FOXA2 alleviates anoikis resistance of A549 cells through promoting the expression of ABCA8. (A) A549 cells were distributed into Control (without treatment), oe-NC and oe-FOXA2 (transfected with oe-FOXA2) groups. The mRNA expression of FOXA2 was detected by RT-qPCR, with GAPDH serving as the internal reference. (B) Gene Expression Profiling Interactive Analysis was used to predict the association between ABCA8 and FOXA2 ($P=5.6x10^{-7}$; R=0.23). (C) ABCA8 protein expression in A549 cells was determined using western blotting, with GAPDH serving as the internal reference. (D) JASPAR was utilized to obtain the predicted binding sites of FOXA2 in ABCA8 promoter region. (E) Relative enrichment of FOXA2 in the promoter region of ABCA8 was evaluated using a chromatin immunoprecipitation assay. (F) Dual-luciferase reporter assay was performed to validate the binding of FOXA2 and ABCA8. (G) A549 cells (suspension culture) were divided into Control (without treatment), sh-NC (transfected with sh-NC) and sh-ABCA8 (transfected with sh-ABCA8) groups. The mRNA expression of ABCA8 was measured using RT-qPCR, with GAPDH serving as the internal reference. (H) A549 cells were assigned to Control (without treatment), sh-ABCA8 (transfected with sh-ABCA8), oe-FOXA2 (treated as before) and oe-FOXA2 + sh-ABCA8 (transfected with oe-FOXA2 and sh-ABCA8) groups. Confocal microscopy images were obtained from a microscope (magnification, x100; scale bar, 100 μm). (I) Viability of A549 cells (suspension culture) was monitored using an MTT assay. **P<0.01 and ***P<0.001. FOXA2, forkhead box protein A2; ABCA8, ATP binding cassette subfamily A member 8; sh-, short hairpin; NC, negative control; oe-, overexpression; RT-qPCR; reverse transcription-quantitative PCR.

FOXA2 alleviates anoikis resistance of A549 cells through promoting the expression of ABCA8. FOXA2 was considered as the upstream transcription factor of ABCA8 after analysis and experimental validation of their association. Transfection efficiency of oe-FOXA2 was examined by RT-qPCR and the data revealed FOXA2 mRNA level was increased 1-fold by oe-FOXA2 (P=0.0003; Fig. 4A). By searching GEPIA, it was determined that ABCA8 was positively correlated with FOXA2 ($P=5.6x10^{-7}$; R=0.23, Fig. 4B). Western blotting was used for determination of ABCA8 expression in A549 cells and the results elucidated that relative protein expression of ABCA8 was significantly increased by 0.8-fold after transfection with oe-FOXA2 (P=0.0013, Fig. 4C). Furthermore, JASPAR was employed to predict the binding sites of FOXA2 to ABCA8 (Fig. 4D). ChIP and dual-luciferase reporter assays were conducted to test the binding of FOXA2 and ABCA8. It was observed that FOXA2 was enriched in the promoter of ABCA8 (P<0.0001; Fig. 4E). In addition, the outcomes of dual-luciferase reporter assay revealed that relative luciferase activity was ~3-fold higher in WT-pcDNA-FOXA2 compared with that of the WT-empty vector (P=0.0004; Fig. 4F), while no significant difference was found in MUT groups (Fig. 4F). Sh-ABCA8 reduced ABCA8 expression in A549 cells by ~50% (P=0.0003; Fig. 4G), indicating successful transfection. The aggregation of A549 cells was promoted after transfection of sh-ABCA8, whereas oe-FOXA2 weakened the effect of sh-ABCA8 (Fig. 4H). In addition, oe-FOXA2 counteracted the promoting role of sh-ABCA8 in A549 cell viability (P=0.0023;

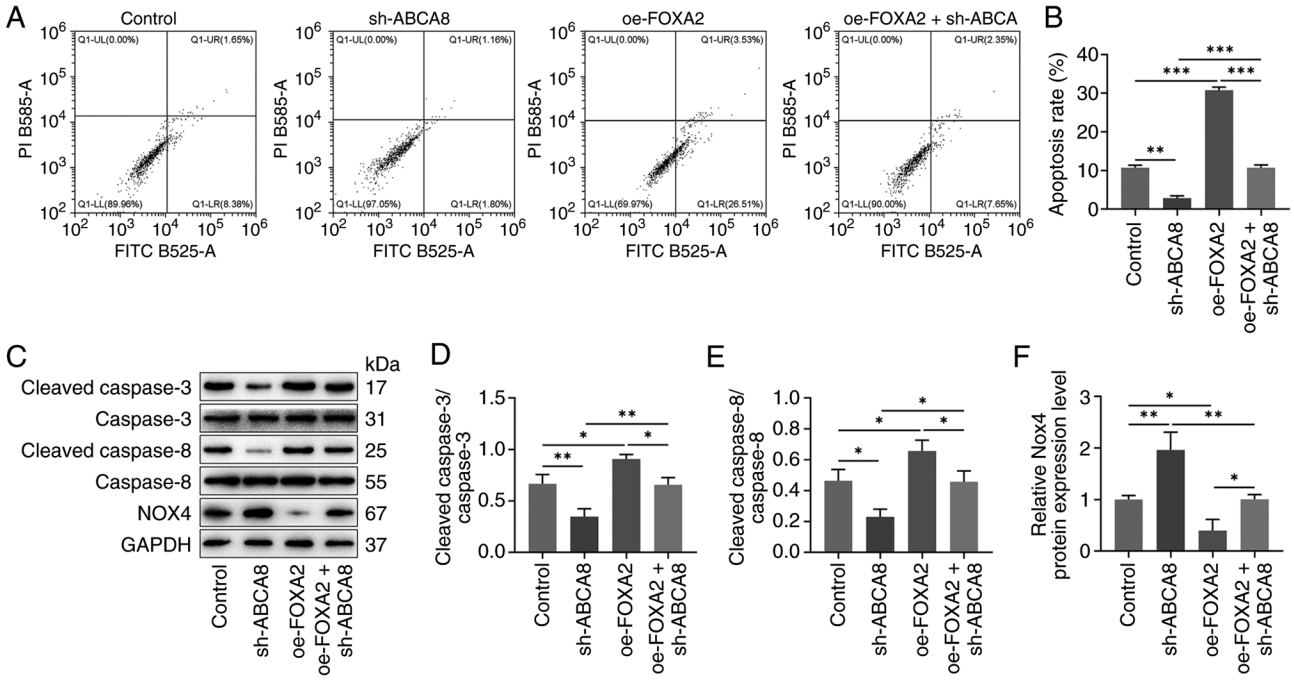

Figure 5. Effect of knocking down ABCA8 or overexpressing FOXA2 on the apoptosis rate and the expression of apoptosis-associated proteins. (A) Flow cytometry was employed to monitor and (B) quantify apoptosis in A549 cells (suspension culture). (C) Western blotting was used to measure (D) cleaved-caspase3, caspase3, (E) cleaved-caspase8, caspase8 and (F) NOX4 protein expression levels in A549 cells (suspension culture), with GAPDH serving as the internal reference. Data are presented as the mean ± SD (n=3). There were three biological replicates in each experimental group. *P<0.05, **P<0.01 and ***P<0.001. FOXA2, forkhead box protein A2; ABCA8, ATP binding cassette subfamily A member 8; NOX4, nicotinamide adenine dinucleotide phosphate oxidase 4; sh-, short hairpin; NC, negative control; oe-, overexpression.

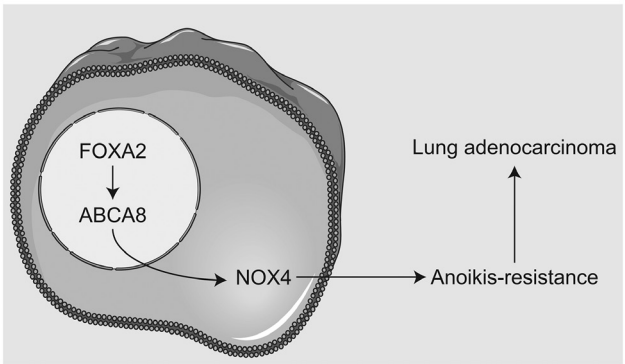

Figure 6. Schematic model of the FOXA2/ABCA8/NOX4 axis in regulating anoikis. FOXA2, forkhead box protein A2; ABCA8, ATP binding cassette subfamily A member 8; NOX4, nicotinamide adenine dinucleotide phosphate oxidase 4.

Fig. 4I). Flow cytometry data indicated that the apoptosis rate was decreased after transfection with sh-ABCA8 (P<0.0001; Fig. 5A and B), which was reversed by oe-FOXA2 (P<0.0001; Fig. 5A and B). Western blotting results further illustrated that sh-ABCA8 inhibited cleaved-caspase3 and cleaved-caspase8 protein expressions and promoted NOX4 expression (P=0.0029, P=0.0116 and P=0.0025; Fig. 5C-F), which was offset by oe-FOXA2 (P=0.0035, P<0.0001 and P=0.0026; Fig. 5C-F). Overall, these results indicated that FOXA2 promoted anoikis of A549 cells by upregulating the expression of ABCA8. Collectively, these findings support a model whereby FOXA2 upregulates ABCA8, which suppresses NOX4 and alleviates anoikis resistance (Fig. 6).

Discussion

ABCA8 belongs to the ABC transporter protein superfamily, whose downregulation is associated with poor prognosis, tumorigenesis and metastasis (20). In previous years, more attention has been paid to the marked effect of ABCA8 on certain cancer types. ABCA8 is regarded as a prognostic biomarker for gastric adenocarcinoma, exhibiting relation to immune infiltration, especially in M2 macrophages (9). ABCA8 overexpression inhibits breast cancer cell proliferation by regulating the AMPK/mTOR signaling pathway (31). ABCA8 is lowly expressed in LUAD and associated with overall survival of patients with LUAD (14); further, ABCA8 suppresses the proliferation of LUAD cells (5). Based on bioinformatic analysis, FOXA2 was identified as an upstream transcription factor of ABCA8. FOXA2 deficiency is frequently observed in NSCLC, the main mechanism of which is epigenetic silencing through promoter hypermethylation (32). FOXA2 also acts as a tumor suppressor of lung cancer metastasis by inhibiting Slug gene expression and the EMT process (33). However, the specific role of FOXA2 as a transcription factor in LUAD remains to be eluidates. In the present study, ABCA8 and FOXA2 mRNA levels were significantly reduced in patients with LUAD and in A549 cells. Normal epithelial cells are sensitive to anoikis, whereas cancer cells are usually resistant to anoikis (34). To compare anoikis sensitivity, immortalized normal bronchial epithelial cells (BEAS-2B) and lung cancer cells (A549) were used.

Anoikis, a type of programmed cell death triggered by cell detachment from the extracellular matrix, is an important

defense against the colonization of distant organs (7). Both anchorage-dependent growth and EMT are associated with anoikis resistance and are important steps in cancer progression and metastatic colonization (35). An increasing number of studies on mechanisms related to anoikis resistance have attracted attention. For example, nuclear MYH9 overexpression promotes CTNNB1 expression and enhance anoikis resistance in gastric cancer (36). Glutamate dehydrogenase 1-mediated reprogramming of glutaminolysis enhances anoikis resistance in LKB1-deficient lung cancer and promotes tumor metastasis (19). Yet, additional information is still needed regarding the genes and pathways that mitigate anoikis resistance in LUAD. As aforementioned, NOX4 is a reactive oxygen species-generating enzyme and silencing of NOX4 attenuated Src expression and enhanced anoikis in lung cancer cells (7). TGF-β mediates the EMT process through the NOX4 signaling pathway, thus promoting lung cancer metastasis (37). The present study analyzed and obtained a negative correlation between ABCA8 and NOX4 in LUAD and accordingly speculated and determined *in vitro* that ABCA8 overexpression could reduce anoikis resistance in LUAD by inhibiting NOX4 expression. Suspension culture of A549 cells has been utilized to induce anoikis, as this method blocks cell adhesion to the extracellular matrix (38). The present results showed that NOX4 expression was elevated in suspended A549 cells and was reduced in A549 cells after oe-ABCA8 transfection. Concurrently, oe-ABCA8 reversed the effects of oe-NOX4 on enhancing cell aggregation, promoting cell viability, dampening apoptosis, decreasing cleaved-caspase3 level and promoting NOX4 expression in suspended A549 cells. This evidence suggested that ABCA8 can negatively regulate NOX4 to ameliorate anoikis resistance in LUAD cells. Suspended cells that form multicellular aggregates exhibit a stronger anoikis resistance than single cells (39). In the present study, the degree of cell aggregation served as one of the indicators to measure anoikis resistance.

Since FOXA2 has been identified as an upstream transcription factor of ABCA8, their association was further determined. ChIP assay results suggested that FOXA2 was enriched in the ABCA8 promoter region. The dual-luciferase reporter assay data showed that FOXA2 bound to the promoter region of ABCA8. In addition, FOXA2 was positively correlated with ABCA8 in LUAD according to GEPIA analysis outcomes and western blotting results demonstrated that oe-FOXA2 promoted ABCA8 protein expression. This indicated that FOXA2 can positively regulate ABCA8. Reportedly, oe-FOXA2 can reduce the ERK phosphorylation level, which in turn inhibits NOX4 expression (15). The present experimental data determined that oe-FOXA2 abrogated sh-ABCA8-induced enhancement of cell aggregation, activation of cell vitality, reduction of apoptosis rate, downregulation of cleaved caspase3 and upregulation of NOX4 in suspension cultured A549 cells.

However, the present study exhibits a number of limitations. First, the present study primarily used cell culture models to investigate the roles of FOXA2 and ABCA8 in tumor resistance, which may not fully replicate the complexity of the *in vivo* tumor microenvironment, systemic drug responses or the full metastatic cascade *in vivo*. Future studies employing *in vivo* metastasis models, such as tail vein injection or orthotopic implantation, will be important in validating the functional importance of this axis in suppressing lung colonization and distant metastasis within a complex physiological microenvironment. Furthermore, while the present study established ABCA8 as a key downstream effector that suppresses NOX4, the precise molecular mechanism by which this transporter protein regulates NOX4 expression potentially through intermediary signals (including ROS) or kinases (such as ERK) remains to be determined and is an important focus for future investigations. Finally, despite the established alterations in expressions of FOXA2, ABCA8 and NOX4 in a number of LUAD cell lines (H1299 and H1975), in-depth mechanistic studies remain predominantly confined to the A549 model. Future research needs to further demonstrate the regulatory network of this pathway in more models.

In conclusion, the present findings established a novel mechanistic association whereby FOXA2-driven ABCA8 transcription sensitizes cancer cells to anoikis by inhibiting NOX4 signaling, thereby inhibiting metastatic dissemination. The findings provide a novel therapeutic avenue for targeting tumor metastasis in LUAD. In therapeutic applications, restoring FOXA2/ABCA8 function or directly inhibiting NOX4 activity could be combined with existing immunotherapies to overcome drug resistance and suppress metastasis. In clinical translation, low expression levels of FOXA2 and ABCA8 may serve as prognostic biomarkers for identifying high-risk patients with metastatic lung cancer.

Acknowledgements

Not applicable.

Funding

No funding was received.

Availability of data and materials

The data generated in the present study are included in the figures and/or tables of this article.

Authors' contributions

NNH and LL performed high-throughput sequencing experiments and performed the bioinformatics analysis. JQH analyzed and interpreted data and wrote the manuscript. LFL designed the study. MMP performed the literature review. MMP and JH were responsible for data acquisition, data analysis and interpretation, they also assisted in the creation of charts and literature review, and participated in the final review and proofreading of the manuscript. LFL, MMP and JH confirm the authenticity of all the raw data. All authors read and approved the final version of the manuscript.

Ethics approval and consent to participate

Not applicable.

Patient consent for publication

Not applicable.

Competing interests

The authors declare that they have no competing interests.

References

1. Bray F, Laversanne M, Sung H, Ferlay J, Siegel RL, Soerjomataram I and Jemal A: Global cancer statistics 2022: GLOBOCAN estimates of incidence and mortality worldwide for 36 cancers in 185 countries. CA Cancer J Clin 74: 229-263, 2024.
2. Liang G, Meng W, Huang X, Zhu W, Yin C, Wang C, Fassan M, Yu Y, Kudo M, Xiao S, *et al*: miR-196b-5p-mediated downregulation of TSPAN12 and GATA6 promotes tumor progression in non-small cell lung cancer. Proc Natl Acad Sci USA 117: 4347-4357, 2020.
3. Song JQ, Wang X, Zeng ZM, Liang PA, Zhong CY and Liu AW: Efficacy of PD-1 inhibitors combined with Anti-angiogenic therapy in driver gene mutation negative Non-Small-cell lung cancer with brain metastases. Discov Med 35: 321-331, 2023.
4. Zuo Y, Shen W, Wang C, Niu N and Pu J: Circular RNA Circ-ZNF609 promotes lung adenocarcinoma proliferation by modulating miR-1224-3p/ETV1 signaling. Cancer Manag Res 12: 2471-2479, 2020.
5. Rotte A: Combination of CTLA-4 and PD-1 blockers for treatment of cancer. J Exp Clin Cancer Res 38: 255, 2019.
6. Miller KD, Siegel RL, Lin CC, Mariotto AB, Kramer JL, Rowland JH, Stein KD, Alteri R and Jemal A: Cancer treatment and survivorship statistics, 2016. CA Cancer J Clin 66: 271-289, 2016.
7. Li Y, Yang Y, Ma Q, Cheng H, Wang H, Ma C, Li F, Zhao S, Li X, Qi Y and Gu Z: HNRNPK/CLCN3 axis facilitates the progression of LUAD through CAF-tumor interaction. Int J Biol Sci 18: 6084-6101, 2022.
8. Liu WJ, Wang L, Zhou FM, Liu SW, Wang W, Zhao EJ, Yao QJ, Li W, Zhao YQ, Shi Z, *et al*: Elevated NOX4 promotes tumorigenesis and acquired EGFR-TKIs resistance via enhancing IL-8/PD-L1 signaling in NSCLC. Drug Resist Updat 70: 100987, 2023.
9. Guo Y, Wang ZW, Su WH, Chen J and Wang YL: Prognostic value and immune infiltrates of ABCA8 and FABP4 in stomach adenocarcinoma. Biomed Res Int 2020: 4145164, 2020.
10. Wang Y, Cheng S, Fleishman JS, Chen J, Tang H, Chen ZS, Chen W and Ding M: Targeting anoikis resistance as a strategy for cancer therapy. Drug Resist Updat 75: 101099, 2024.
11. Dong B, Gu Y, Sun X, Wang X, Zhou Y, Rong Z, Zhang J, Shi X, Zhang Z, He X, *et al*: Targeting TUBB3 suppresses anoikis resistance and bone metastasis in prostate cancer. Adv Healthc Mater 13: e2400673, 2024.
12. D'Amore T, Bravoco D, Di Paola G, Albano F, Brancaccio M, Sabato C, Cesta G, Zolfanelli C, Lauciello V, Falco G and Mazzone P: Anoikis resistance in gastric cancer: A comprehensive review. Cell Death Dis 16: 528, 2025.
13. Wang F, Su Q and Li C: Identidication of novel biomarkers in non-small cell lung cancer using machine learning. Sci Rep 12: 16693, 2022.
14. Yang Y, Liu X, Wang X, Zhang J, Li S and Ma X: Comprehensive analysis of ABCA family members in lung adenocarcinoma with prognostic values. Mol Biotechnol 4: 1441-1453, 2022.
15. Xu YJ, Huo YC, Zhao QT, Liu JY, Tian YJ, Yang LL and Zhang Y: NOX4 promotes tumor progression through the MAPK-MEK1/2-ERK1/2 axis in colorectal cancer. World J Gastrointest Oncol 16: 1421-1436, 2024.
16. Hu T, Li Z, Gao CY and Cho CH: Mechanisms of drug resistance in colon cancer and its therapeutic strategies. World J Gastroenterol 22: 6876-6889, 2016.
17. Bharathiraja P, Yadav P, Sajid A, Ambudkar SV and Prasad NR: Natural medicinal compounds target signal transduction pathways to overcome ABC drug efflux transporter-mediated multidrug resistance in cancer. Drug Resist Updat 71: 101004, 2023.
18. Ji N, Li H, Zhang Y, Li Y, Wang P, Chen X, Liu YN, Wang JQ, Yang Y, Chen ZS, *et al*: Lansoprazole (LPZ) reverses multidrug resistance (MDR) in cancer through impeding ATP-binding cassette (ABC) transporter-mediated chemotherapeutic drug efflux and lysosomal sequestration. Drug Resist Updat 76: 101100, 2024.
19. Jin L, Chun J, Pan C, Kumar A, Zhang G, Ha Y, Li D, Alesi GN, Kang Y, Zhou L, *et al*: The PLAG1-GDH1 axis promotes anoikis resistance and tumor metastasis through CamKK2-AMPK signaling in LKB1-deficient lung cancer. Mol Cell 69: 87-99.e7, 2018.
20. Cui Y, Liang S, Zhang S, Zhang C, Zhao Y, Wu D, Wang J, Song R, Wang J, Yin D, *et al*: ABCA8 is regulated by miR-374b-5p and inhibits proliferation and metastasis of hepatocellular carcinoma through the ERK/ZEB1 pathway. J Exp Clin Cancer Res 39: 90, 2020.
21. Kim HJ, Kim D, Yoon H, Choi CS, Oh YS and Jun HS: Prevention of oxidative Stress-induced pancreatic beta cell damage by Broussonetia Kazinoki Siebold fruit extract via the ERK-Nox4 pathway. Antioxidants (Basel) 9: 406, 2020.
22. Kim H, Sung JY, Park EK, Kho S, Koo KH, Park SY, Goh SH, Jeon YK, Oh S, Park BK, *et al*: Regulation of anoikis resistance by NADPH oxidase 4 and epidermal growth factor receptor. Br J Cancer 116: 370-381, 2017.
23. Chandrashekar DS, Karthikeyan SK, Korla PK, Patel H, Shovon AR, Athar M, Netto GJ, Qin ZS, Kumar S, Manne U, *et al*: UALCAN: An update to the integrated cancer data analysis platform. Neoplasia 25: 18-27, 2022.
24. Zhang Q, Liu W, Zhang HM, Xie GY, Miao YR, Xia M and Guo AY: hTFtarget: A comprehensive database for regulations of human transcription factors and their targets. Genomics Proteomics Bioinformatics 18: 120-128, 2020.
25. Bao J, Li D, Wang L, Wu J, Hu Y, Wang Z, Chen Y, Cao X, Jiang C, Yan W and Xu C: MicroRNA-449 and microRNA-34b/c function redundantly in murine testes by targeting E2F transcription factor-retinoblastoma protein (E2F-pRb) pathway. J Biol Chem 287: 21686-21698, 2012.
26. Yang Z, Wang T, Wu D, Min Z, Tan J and Yu B: RNA N6-methyladenosine reader IGF2BP3 regulates cell cycle and angiogenesis in colon cancer. J Exp Clin Cancer Res 39: 203, 2020.
27. Lee CT, Li R, Zhu L, Tribble GD, Zheng WJ, Ferguson B, Maddipati KR, Angelov N and Van Dyke TE: Subgingival microbiome and Specialized Pro-Resolving lipid mediator pathway profiles are correlated in periodontal inflammation. Front Immunol 12: 691216, 2021.
28. Song Z, Xiang X, Li J, Deng J, Fang Z, Zhang L and Xiong J: Ruscogenin induces ferroptosis in pancreatic cancer cells. Oncol Rep 43: 516-524, 2020.
29. Guo X, Wang Z, Sun Q, Sun C, Hua H and Huang Q: The inhibitory effect of microRNA-1827 on anoikis resistance in lung adenocarcinoma A549 cells via targeting caveolin-1. Acta Biochim Biophys Sin (Shanghai) 52: 1148-1155, 2020.
30. Jiao Y, Li Y, Zhang J, Zhang S, Zha Y and Wang J: RRM2 alleviates doxorubicin-induced Cardiotoxicity through the AKT/mTOR signaling pathway. Biomolecules 12: 299, 2022.
31. Lv C, Yang H, Yu J and Dai X: ABCA8 inhibits breast cancer cell proliferation by regulating the AMP activated protein kinase/mammalian target of rapamycin signaling pathway. Environ Toxicol 37: 1423-1431, 2022.
32. Basseres DS, D'Alò F, Yeap BY, Löwenberg EC, Gonzalez DA, Yasuda H, Dayaram T, Kocher ON, Godleski JJ, Richards WG, *et al*: Frequent downregulation of the transcription factor Foxa2 in lung cancer through epigenetic silencing. Lung Cancer 77: 31-37, 2012.
33. Jin S, He J, Zhou Y, Wu D, Li J and Gao W: LncRNA FTX activates FOXA2 expression to inhibit non-small-cell lung cancer proliferation and metastasis. J Cell Mol Med 24: 4839-4849, 2020.
34. Kim YN, Koo KH, Sung JY, Yun UJ and Kim H: Anoikis resistance: An essential prerequisite for tumor metastasis. Int J Cell Biol 2012: 306879, 2012.
35. Paoli P, Giannoni E and Chiarugi P: Anoikis molecular pathways and its role in cancer progression. Biochim Biophys Acta 1833: 3481-3498, 2013.
36. Ye G, Yang Q, Lei X, Zhu X, Li F, He J, Chen H, Ling R, Zhang H, Lin T, *et al*: Nuclear MYH9-induced CTNNB1 transcription, targeted by staurosporin, promotes gastric cancer cell anoikis resistance and metastasis. Theranostics 10: 7545-7560, 2020.
37. Ma M, Shi F, Zhai R, Wang H, Li K, Xu C, Yao W and Zhou F: TGF-β promote epithelial-mesenchymal transition via NF-κB/NOX4/ROS signal pathway in lung cancer cells. Mol Biol Rep 48: 2365-2375, 2021.
38. Zhong X and Rescorla FJ: Cell surface adhesion molecules and adhesion-initiated signaling: understanding of anoikis resistance mechanisms and therapeutic opportunities. Cell Signal 24: 393-401,2012.
39. Zhang Y, Lu H, Dazin P and Kapila Y: Squamous cell carcinoma cell aggregates escape suspension-induced, p53-mediated anoikis: Fibronectin and integrin alphav mediate survival signals through focal adhesion kinase. J Biol Chem 279: 48342-48349, 2004.